

## COMBINED VACUUM-ARC HARDENING OF FRICTIONAL UNIT COMPONENTS

*V.A. Belous, I.G. Yermolenko, Yu.A. Zadneprovsky, N.S. Lomino*  
*National Science Center "Kharkov Institute of Physics and Technology"*  
*Kharkov, Ukraine*

*E-mail: yaz@kipt.kharkov.ua*

For increasing the service life of steel components that form a friction pair and are operated under conditions of dynamic loads, elevated temperatures and corrosive media, the process of working contact surface modification has been developed with the use of the vacuum-arc technique. The process has been realized in a two-stage technological cycle, including hardening of the base material by ion-plasma nitriding that replaces effectively the "furnace" nitriding, and a subsequent deposition of protective coatings Mo-N (molybdenum nitride) and Ti-N (titanium nitride). Various physical properties of the modified samples (microhardness depth profiles, as well as structure peculiarities of nitrided layers and nitride coatings) have been investigated as functions of the parameters of the process under development. Comparative laboratory tests of service characteristics (abrasion/corrosion resistances) of the components have been made, and an essential improvement of these characteristics has been demonstrated for the modified surfaces.

The development of turbine engineering makes necessary the improvement in the reliability of turbine control systems, in particular, the components of the steam distribution unit. The structure of this unit in the turbine K-325 comprises the elements that form the friction pair, operate under dynamic loads, and are subject to abrasion/corrosion wears, too. Fig. 1 illustrates some of those elements.

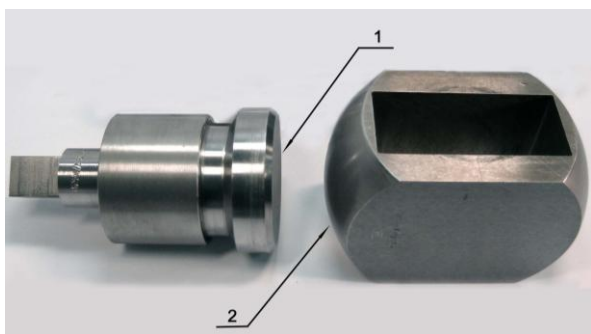


Fig. 1. Friction pair elements: "Support" (1) and "Joint" (2). (The arrows show the contacting areas)

At plant conditions, for hardening of the mentioned unit elements it was customary to use "furnace" nitriding [1]. In accordance with the technical requirements of PJSC "Turboatom" to increase the wear resistance of the friction surfaces of the rotating "Support" and "Joint". That protective coatings have proposed that thin (up to 10  $\mu\text{m}$ ) layers of very hard nitride-based coatings, well-proven earlier in all kinds of service applications [2], should be used. However, since the "furnace" nitriding had appeared incompatible with a subsequent vacuum-arc deposition of coatings because of their poor adherence, then, as an alternative, the method of ion nitriding in the plasma created by the two-step vacuum-arc discharge (TSVAD) was used [3–4].

During deposition of wear-resistant coatings on the bumpy surface of the «Joint», the molybdenum nitride film was formed, while on the concave surface of the "Support" the titanium nitride coating was formed. (In

this particular case, the deposition of coatings having different compositions was caused by the necessity to overcome the setting-up effect typical for materials of the same composition). The two successive stages (nitriding + protective coating deposition) were realized in a single technological process with one-time loading of the elements into the vacuum chamber.

### STAGES OF ST.25CrMoVa MODIFICATION

Fig. 2 shows the characteristic temperature-time curve for the element at different stages of its surface modification. The limiting heating temperature in the TSVAD plasma and during metal ion bombardment was determined (at a fixed heat removal to the element holder) by the applied potential value and the duration time of each of the process stages. The stage duration was also dependent on the mass of the elements to be hardened.

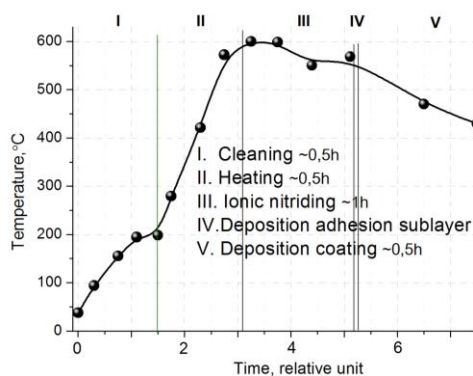


Fig. 2. Different stages of sample surface modification process in the temperature-time coordinates

In the "Cleaning" stage, the sample was exposed to argon plasma created by means of the TSVAD. The use of this stage, being the result of low-energy action of the discharge plasma on the processed surface, has allowed us to avoid local discharge positioning that may lead to faulty production. The next stage, conditionally called "Heating", took place as the unit element was bombarded by metal (titanium/molybdenum) ions at a

higher accelerating potential, and it terminated upon attaining the working temperature of nitriding. In the “Ion nitriding” stage, nitrogen was let in the chamber volume, and the two-step vacuum-arc discharge was initiated. As the run of the curve in Fig. 2 shows, by the end of the stage a certain temperature drop (within 10%) of the processed surfaces occurred. The current density of gaseous ions, accelerated by the -500 V potential applied to the unit element, was found to be  $\sim 1 \text{ mA/cm}^2$ . The duration of the nitriding stage was no more than one hour.

The “Sublayer deposition” stage followed immediately after the nitriding of the base material (st.25CrMoVa) was completed. A thin ( $\leq 2 \mu\text{m}$ ) titanium or molybdenum layer was deposited by the vacuum-arc method on the surface of the “Support” or the “Joint”, respectively. This provided a high degree of adherence to thicker (up to  $10 \mu\text{m}$ ) nitride layers of the metals deposited at the next stage of surface modification.

The process of integrated hardening of the unit element was completed by the deposition of the coating based on titanium/molybdenum nitrides. At this stage, a gradual temperature decrease took place, since the energy contribution from the deposited ions at a lower potential applied to the element, did not compensate the heat removal losses.

The modification of the “Support” steel surface through deposition of the Ti-N coating was realized by using a similar pre-nitriding procedure as that applied for the “Joint” with the Mo-N coating.

### OPTIMIZATION OF COATING DEPOSITION MODES

When forming coatings of different compositions (MoN and TiN), the gaseous pressure value was chosen out of the necessity to provide approximately equal microhardness values  $H_{\mu}$  for these coatings. This requirement was dictated by the peculiarities interaction of hardened element performance in the friction pair under symmetrical contact loads.

The coating deposition process was also optimized when choosing the substrate bias potential. This parameter of the deposition process had an effect on the characteristics of the both coatings. Thus, the maximum hardness values for the Mo-N coatings were obtained at minimum bias potentials; that corresponded to “colder” deposition conditions. The increase of the potential, and hence, of temperature in the condensation region led to more equilibrium conditions of deposition; and in this case the microhardness of the deposited coatings was reduced (Table 1).

Table 1

Coating microhardness at different bias potentials ( $P_{N_2} = (1.5 \dots 2) \cdot 10^{-3} \text{ Torr}$ )

U, V	$H_{\mu}$ , GPa	
	Mo-N	Ti-N
50	33.9	27.2
60	29	26.2
100	23.5	24.5

It should be noted that some modes of Mo-N coating deposition are typified by the appearance of microcracks. The titanium nitride coatings exhibited no cracking in the whole range of deposition parameters under study. That may testify to a lower level of internal stresses in these coatings.

The absence of cracks on the coating surfaces is the necessary, but insufficient criterion of fitness for service applications. Though having rather high internal stress levels, very hard coatings of Mo-N composition may also exhibit cracking at their relaxation with time and (or) under loads, which has a detrimental effect on their performance characteristics. Therefore, the final choice of the mode of coating deposition, and hence, of the optimum  $H_{\mu}$  value, was made on the basis of the performance test results.

### DEPTH DISTRIBUTION OF NITROGEN CONCENTRATIONS IN STEEL

For measuring the hardened layer thickness, metallographic sections of the processed samples were prepared. In the measurements, the indentation technique aided by the Nanoindenter G200 was used. The initial microhardness on the non-nitrided surface of st.25CrMoVa samples was determined to be no more than 3.5 GPa.

Fig. 3 shows the depth distributions of the nitrogen content and the microhardness for two samples (one – nitrided only, the other – subjected to nitriding + a subsequent Mo-N coating deposition. (The nitrogen concentration profiles were measured with a  $10 \mu\text{m}$  step on the electron microscope, using the X-ray fluorescence analysis).

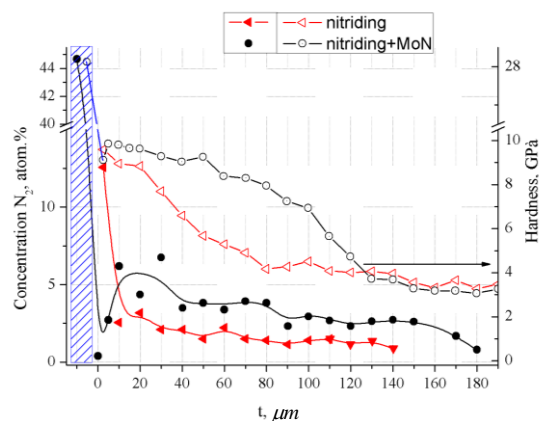


Fig. 3. Depth profiles of nitrogen concentration and microhardness for the processes of ionic nitriding and nitriding plus Mo-N coating deposition. (The hatching defines the region related to the coating)

The increased (up to 45 at.%) nitrogen content of the deposited coating (shaded region in Fig. 3) is attributed to the synthesis of the corresponding molybdenum nitride phases, i.e., to the stable-state presence of nitrogen in the steel. It is just the presence of these phases that explains the higher hardness of the deposited nitride layer. Under the Mo-N coating, there was a thin intermediate Mo layer deposited for improving the adhesive properties under higher vacuum conditions ( $P \sim 10^{-5} \text{ Torr}$ ); and the points on the curve in Fig. 3 just refer to this layer having the minimum nitrogen

concentration. As is seen from the figure, the spatial extent ( $\sim 10 \mu\text{m}$ ) of the dip, related to the mentioned minimum, substantially exceeds the thickness of the deposited Mo layer. This is possibly due to the processes of steel surface denitriding that occur during surface heating under ion bombardment, which is used before deposition of the molybdenum interlayer.

It also follows from Fig. 3 that the nitrogen concentration and the depth of its penetration into the substrate material for the samples subjected to different ion-plasma treatments are essentially different. The coating-bearing nitrided samples exhibit higher concentrations of nitrogen and its greater penetration depths than the samples that were subjected to nitriding only. As a result of the process of ion-plasma nitriding, the nitrogen is concentrated in the near-surface layer of the steel substrate to a depth up to  $20 \mu\text{m}$ , whereas at depths up to  $\sim 80$  to  $100 \mu\text{m}$  the nitrogen concentration is reduced to a level of  $\sim 2.5 \text{ at.}\%$ .

Considering that the process of nitride coating deposition was carried out in the nitrogen atmosphere, and with substrate heating (see Fig. 2), it was necessary to verify whether the process of substrate nitriding has ceased or still continued at the stage of coating deposition. For this purpose, we have investigated the nitrogen depth profile through the use of the metallographic section of the steel sample that underwent coating deposition but without the stage of prenitriding. Fig. 4 shows the data of microprobe X-ray fluorescence analysis related to the behavior of the main substrate component, Fe, and to the plasma flow components (Mo and N) participating in the process of coating deposition.

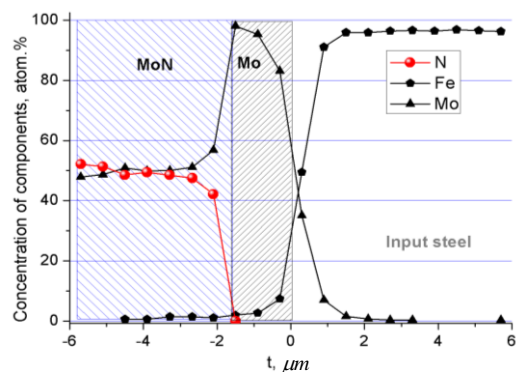


Fig. 4. Distributions of Mo, N and Fe components in the metallographic section of the sample with Mo ( $2 \mu\text{m}$ ) and Mo-N ( $4.5 \mu\text{m}$ ) layers

We call your attention to the component distribution in the intermediate layer adjacent partially to the  $\sim 2 \mu\text{m}$  thick substrate surface and partially to the Mo layer deposited on the substrate surface ( $\sim 1.5 \mu\text{m}$  in thickness). The interlayer exhibits the concentration distribution of the Fe atoms as being the main components of the substrate, and the deposited Mo atoms. The existence of this layer can be explained in terms of the processes of ion mixing, which take place as the steel surface is exposed to molybdenum ions. The ion mixing results from partial sputtering of the substrate atoms, their ionization in the near-surface layer and subsequent return to the surface under the

action of the applied negative potential. As regards the nitrogen atoms in the Mo sublayer, they were not observed there, i.e., there was no penetration of nitrogen into the steel substrate at the stage of vacuum-arc coating deposition. In turn, the Mo layer is a barrier for the escape of nitrogen already absorbed by the substrate surface both at the stage of Mo deposition and the stage of application of the Mo-N coating. As the deposition processes are carried out, the samples continue to heat, and the concentration of nitrogen atoms in the steel substrate of the sample, formed in the stage of nitriding, gets redistributed deep into the metal.

In this way, the two-stage process of ion-plasma treatment has resulted in the formation of the layer of improved hardness ( $H \sim 5 \text{ GPa}$ ) on the steel sample surface to a depth of  $100 \mu\text{m}$ , and the nitride coating with  $H \sim 30 \text{ GPa}$ .

### STRUCTURAL CHARACTERISTICS OF THE MODIFIED LAYERS

Fig. 5 gives the comparative transverse-fracture photographs taken from different samples: initial (1), hardened by ion nitriding (2), and with Mo-N and Ti-N coatings deposited onto the nitrided surface (3).

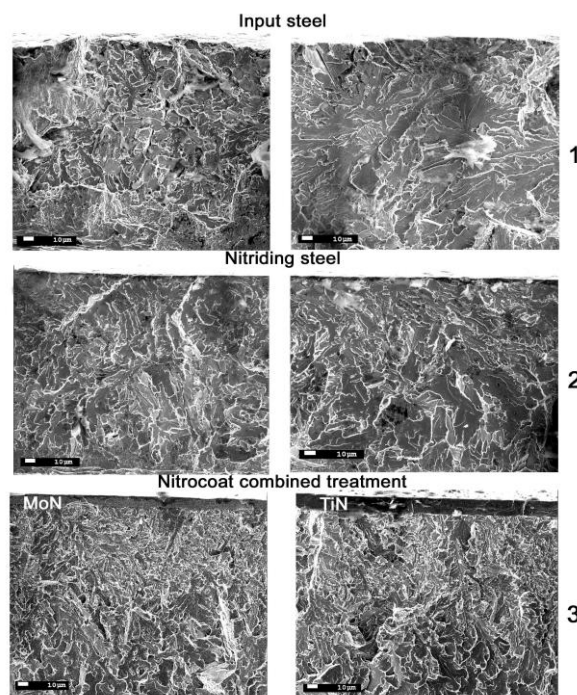


Fig. 5. Transverse fracture pictures: 1 – initial steel st.25CrMoVa; 2 – nitrided steel; 3 – nitrided steel with Ti-N and Mo-N coatings

The pictures were taken using the scanning electron microscope. The structure of the initial steel sample shows the presence of specific grained formations with predominance of large-size grains ( $\sim 100 \mu\text{m}$ ). After ion nitriding (see Fig. 5 (2)) some structure ordering with grain refining to a layer depth of  $\sim 70 \mu\text{m}$  takes place. The essential steel structure rearrangement with grain refinement down to  $1 \dots 3 \mu\text{m}$  (immediately under the coating) and with a tendency of grain coarsening up to  $\sim 10 \mu\text{m}$  is observed at a depth of down to  $\sim 100 \mu\text{m}$  (see Fig. 5 (3)). This behavior of steel structure characteristics reflects the mode of spatial distribution

of nitrogen deep in the metal, and is responsible for the formation of the hardness  $H(t)$  profile (see Fig. 3).

### CRYSTALLOGRAPHIC STUDIES OF THE COATED SAMPLES

The analysis of X-ray spectra taken from the coated samples (Fig. 6) gives the following estimates for the crystal orientations in the obtained coatings. The titanium nitride-based coatings exhibit predominantly a strong reflection (111), which corresponds to the NaCl – type crystalline structure with the parameter  $a = 0.426$  nm and the coherent-scattering region of size  $L \approx 41$  nm. The X-ray spectrum for the molybdenum nitride-based coatings is more complicated. It shows three  $\gamma$ -Mo<sub>2</sub>N lines with the lattice parameter  $a = 0.420$  and the size  $L \approx 11$  nm. Note that the amplitudes of each of the reflections under discussion differ insignificantly from each other.

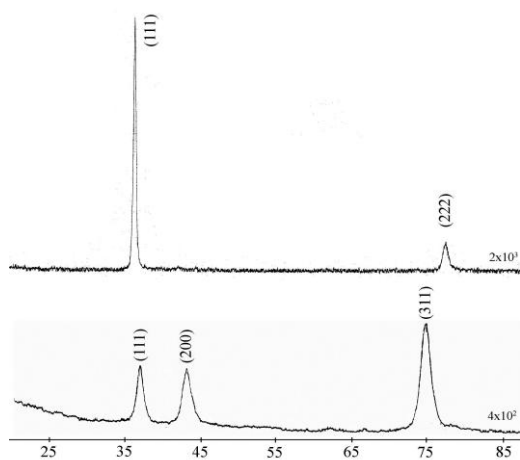


Fig. 6. X-ray patterns of protective coatings based on Ti-N (above) and Mo-N (below)

The differences between the X-ray spectra of Ti-N and Mo-N coatings are also confirmed by structural electrooptical images of fractured samples having coatings of different compositions (Fig. 7).

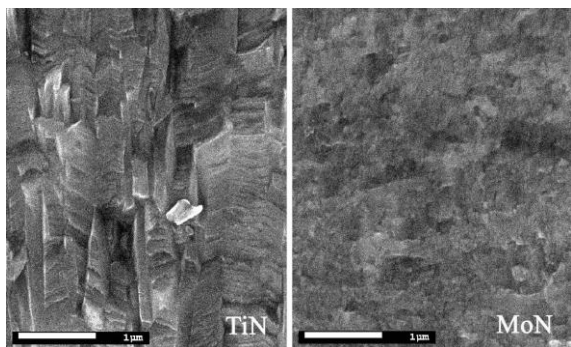


Fig. 7. Electrooptical images of Ti-N and MoN-coatings fractures

In fact, while the photograph of the Ti-N-coating clearly shows the columnar structure of the preferred orientation, the crystallites seen in the fracture of the Mo-N-base coating are smaller-sized, and their preferred orientation is absent.

### INTERNAL STRESSES IN THE COATINGS

The analysis of X-ray spectra taken from the samples with coatings of different compositions has enabled us to estimate the macrodeformational compression stresses in the chosen (optimal) modes of deposition; the obtained results are given in Table 2.

Table 2

Macrodeformational compression stresses and microhardness of the coatings

Coating	Potential displacement, B	$H_{\mu}$ , GPa	Compressive deformation $\varepsilon$ , %
Mo-N	-85	27.8	-1.84
Ti-N	-90	25.8	-0.77

As it follows from the table, the level of the stresses in the Mo-N-base coatings is substantially higher than in the Ti-N-coatings, even though their microhardness values differ insignificantly.

### ADHESIVE CHARACTERISTICS OF THE COATINGS

In principle, the vacuum-arc deposition techniques provide a satisfactory adherence of coatings to the substrate. This is achieved by applying ion-beam cleaning of the base surface done immediately before application of coatings. This cleaning technique not only provides the removal of possible impurities off the surface, but also initiates the process of ion mixing of the sputtered base atoms with the deposited coating atoms.

The ion-plasma nitriding followed by application of protective coatings also provides high adhesion characteristics of the obtained coating-base formation. The good adhesion is additionally contributed by thin (1 to 2  $\mu$ m) intermediate layers of titanium or molybdenum deposited onto the nitrided surface of the base with the use of the same cathodes as the ones used for subsequent Ti or Mo nitride layers.

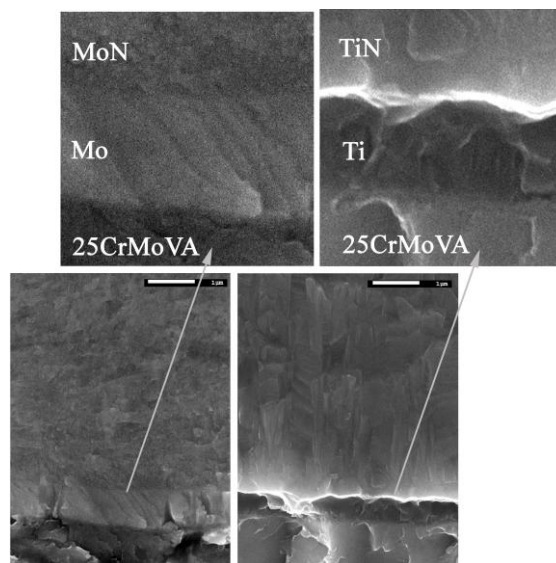


Fig. 8. Transverse fractures of steel samples with deposited layers of metals and their nitrides

Fig. 8 gives the photographs of brittle fractures of the samples having coatings of different compositions.

The attention is drawn to a high degree of consistency the substrate-metal and metal-its nitride interface profiles, this bearing witness to a reasonable level of adhesion.

Fig. 9 presents the photos of the track produced as the diamond indenter passed under increasing load conditions over the surface of the Mo-N-coating, which was deposited onto the steel samples being in the initial and nitrided states. (The total run length of the indenter in the figure is ~ 400 μm). We call your attention to a substantial delay in the onset of cracking (and peeling) of the coating deposited on the nitrided base in comparison with the coating deposited on the initial-state steel.

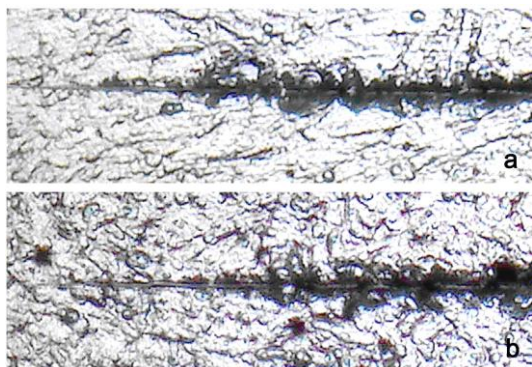


Fig. 9. Mo-N-coated surfaces with track marking of diamond indenter run:  
a – coating on the initial-state steel base;  
b – coating on the nitrided steel

So, the application of the given technique has confirmed the fact of improvement in the adhesive properties of coatings as they are deposited on the nitrided steel base.

### PHYSICAL AND MECHANICAL CHARACTERISTICS OF THE COATINGS

Tables 3 and 4 give the research data on the physical and mechanical characteristics of the obtained Ti-N and Mo-N-coatings, depending on whether the coatings were deposited on the initial surface of steel or on its surface after nitriding.

Table 3  
Physical-and-mechanical properties  
("Micron-Gamma" measurements)

Modified surface	Micro-hardness, GPa	Nano hardness, GPa	Elastic modulus, GPa	H/E
Ti-N	29.7	28.6	451	0.06
Nitriding + Ti-N	28.9	29.2	447	0.065
Mo-N	29.8	30.3	377	0.08
Nitriding + Mo-N	28.5	32.1	439	0.07

Table 4  
Physical-and-mechanical properties  
(G200 and PMT-3 measurements)

Modified surface	H, GPa	E, GPa	H/E
Ti-N	34	436	0.08
Nitriding + Ti-N	36.5	425	0.09
Mo-N	32	308	0.1
Nitriding + Mo-N	38	381	0.1

The investigations were performed using different methods and devices, in particular, the facility "Micron-Gamma" [7] when working with the Vickers indenter (see Table 3), and the devices G200 and PMT-3 at nano- and microindentation (see Table 4). Despite the fact that the two methods give somewhat different results, these differences are insignificant. As it follows from Fig. 3, the process of nitriding has led to an appreciable increase in the hardness of the steel base from 2.7 up to 9 GPa. However, on subsequent deposition of the protective coatings Ti-N and Mo-N, all the  $H_{\mu}$  values measured with one method (see Table 3), and also, the  $H_{\mu}$  and H values measured with the other method (see Table 4), are practically no different from the corresponding values for the coatings deposited on the initial steel surface. This implies that the parameters describing the physical-mechanical characteristics of the coatings (see Tables 3 and 4) are independent of the properties of the base, onto which the coatings were deposited. Surely, this conclusion is valid for relatively thick coatings, when their thickness considerably exceeds the depths of indentation.

The parameter H/E is one of the important characteristics of the material [5]. It characterizes the ability of the material to resist changes in shape and dimensions under deformation. It can be also used for estimating the frictional wear of the material. There are empirical relationships [6], which enable one to define the type of the structural state by using the mentioned parameter. As it is evident from Table 5, the range of H/E values for our Mo-N and Ti-N-coatings varies between 0.06 and 0.08, and that corresponds to fine-crystalline structural condition. In this case, the physical-mechanical properties of the modified layers of different compositions, but appearing to be the contacting pair in the frictional unit, differ insignificantly.

### WEAR RESISTANCE OF THE COATINGS

The wear rates of different coating materials were compared by measuring the parameter  $I_t$ , which is the ratio of the indentation depth to the path length covered by the diamond indenter over the surfaces of the given materials. As it follows from the data given in Table 5, the resistance of the nitride coatings Ti-N and Mo-N to the given wear mode is essentially dependent on what substrate the coatings were deposited. And in the case of the nitrided steel, the linear wear index is lower than that of the coatings deposited on the initial material.

Table 5

Linear wear of different materials

Coating	St.25CrMoVa	Linear wear $I_1, 10^{-7}$
Ti-N	–	0.95
	nitriding	0.52
Mo-N	–	0.75
	nitriding	0.61

### TRIBOLOGICAL CHARACTERISTICS OF THE COATINGS

The comparison of friction coefficients of different materials (Table 6) was carried out using the “Micron-Gamma” facility. The diamond indenter was used as a counterbody; therefore, the friction coefficient values given in Table 6 are relative and can be used only for the purposes of comparison with different materials.

Table 6

Coefficients of diamond indenter friction over different materials at different loads

Coating	St.25CrMoVa	Coefficient of friction, $f_{fr}$		
		Load, g		
		225	375	525
Ti-N	–	0.09	0.09	0.09
	nitriding	0.05	0.06	0.06
Mo-N	–	0.09	0.09	0.09
	nitriding	0.065	0.066	0.07

Note the load independence of the  $f_{fr}$  values listed in the table. In this case, the friction coefficients for the coatings deposited on the nitrided base are substantially lower than those found for the coatings deposited onto the steel base not subjected to nitriding.

### PERFORMANCE CHARACTERISTICS OF THE MODIFIED SAMPLES

To investigate corrosion resistance in the 3% NaCl medium, the potentiometer testing technique was used. Fig. 10 shows the current density  $j$  curves as functions of the potential  $\phi$  for the following samples: initial steel, discharge-nitrided steel, and the nitrided steel having the protective Mo-N and Ti-N-coatings.

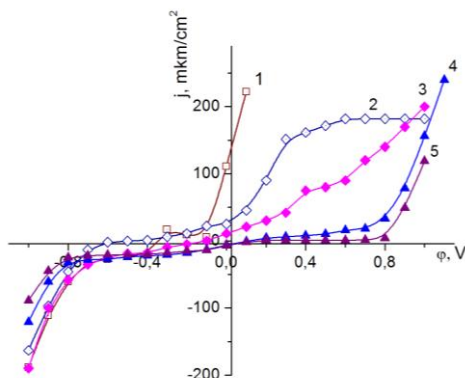


Fig. 10. Current-voltage characteristics of different samples in aggressive medium at corrosion testing: 1 – steel in the initial state; 2 – steel after “furnace” nitriding; 3 – steel after ion-plasma nitriding; 4 – Mo-N-coated nitrided steel; 5 – Ti-N-coated nitrided steel

For comparison, the same figure gives the corrosion test data for the steel subjected to “furnace” nitriding. From the behavior of the  $j(\phi)$  curve for the initial st.25CrMoVa it follows that this material has a low corrosion resistance. The performance of “furnace” or ion-plasma nitriding processes results in improving the anticorrosion properties of steel. Notably that the second of the two mentioned processes has a distinct advantage. However, the highest protective properties against corrosion medium are exhibited by the samples subjected to a combined modification, when the Mo-N or Ti-N-coatings were deposited onto the steel surface that underwent nitriding in the gas-discharge plasma.

Fig. 11 shows the comparative data on the resistance of different samples under abrasive action. The abrasive wear of the coatings was performed with the setup described in ref. [8]; it was estimated by the weight loss of the sample surface exposed to abrasion cycling.

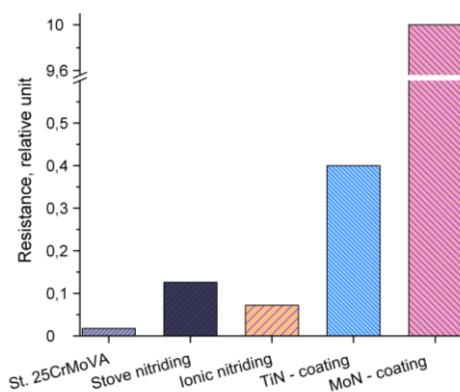


Fig. 11. Abrasive wear of different sample

As can be seen from Fig. 11, the application of the above-discussed processes for modifying the initial steel surface leads to a substantial improvement of its abrasion resistance. Thus, ionic nitriding increases the abrasion resistance by more than an order of magnitude, while the Ti-N-coating deposited on the nitrided steel base increases the resistance of the initial steel by a factor of more than 20, and the Mo-N-coating – by a factor of up to 500.

### CONCLUSIONS

1. To replace the “furnace” nitriding, the method of ion-plasma nitriding of the steel has been offered, which is compatible with a subsequent coating deposition.
2. The pilot process of vacuum ion-plasma nitriding of the surface has been developed for full-scale components forming the friction pair. As a result, layers of improved hardness have been formed on the sample surface to a depth up to 100  $\mu\text{m}$ .
3. Processes of depositing protective Mo-N- and Ti-N-coatings on the nitrided sample surfaces have been investigated. In the selected optimized modes of deposition, coatings with close values of microhardness (at a level of 29 GPa) have been obtained.
4. The process of combined vacuum-arc hardening in a single technological cycle (nitriding + coating) has been developed for full-scale components.
5. Diversified studies on physical characteristics have been made for modified layers applied for protecting working surfaces of the components. The

steel base nitriding results in size reduction of the structure formations, viz., the grain size decreases by an order of magnitude.

6. The use of protective coatings on the nitrated steel surface has provided a substantial improvement in the service characteristics of the hardened samples. Their corrosion resistance has become nearly fivefold higher, while the abrasion resistance has increased by one to two orders of magnitude.

#### REFERENCES

1. Yu.M. Lakhtin, Ya.D. Kogan, G.I. Shpis, et al. *Theory and technology of nitriding*. M.: "Metallurgiya", 1991, 320 p.
2. I.I. Aksyonov, A.A. Andreyev, V.A. Belous, et al. *Vacuum arc. Plasma sources, coating deposition, surface modification*. Kiev: "Naukova Dumka", 2012, 728 p.
3. L.P. Sablev, N.S. Lomino, R.I. Stupak, A.A. Andreyev, A.M. Chikryzhov. Two-step vacuum-arc discharge: characteristics and initiation techniques. // *Reports on the 6<sup>th</sup> International Conference "Equipment and heat treatment technologies for metals and alloys"*. Kharkov: NSC KIPT, 2005, v. 2, p.159-169.
4. A.A. Andreyev, V.M. Shulayev, L.P. Sablev. Steel nitriding in a low-pressure gaseous arc discharge // *PSE*. 2006, v. 4, N 3-4, p. 191-1975.
5. Yu.V. Mil'man. New techniques of micromechanical testing of materials by the local rigid-indenter loading method // *Current materials science of the XXI century*. Kiev: "Naukova Dumka", 1998, p. 637-656.
6. S.A. Firstov, V.F. Gorban', Eh.P. Pechkovsky. *New methodology of processing and analysis of the results of automatic indentation of materials*. Kiev: "Logos", 2009, p. 23.
7. S.R. Ignatovich, I.M. Zakiyev. Universal micro-nanoindentometer "Micron-Gamma" // *Zavodskaya Laboratoriya. Diagnostika Materialov*. 2011, N 1, v. 77, p. 61-67 (in Russian).
8. I.I. Aksyonov, V.A. Belous, Yu.A. Zadneprovsky, V.I. Kovalenko, N.S. Lomino. The effect of small silicon additives on the service characteristics of nitride-titanium coatings // *Voprosy Atomnoj Nauki i Tekhniki. Seriya "Fizika radiatsionnykh povrezhdenij i radiatsionnoe materialovedenie"*. 2011, N 4, p. 145-149 (in Russian).

Статья поступила в редакцию 21.03.2016 г.

### КОМБИНИРОВАННОЕ УПРОЧНЕНИЕ ДЕТАЛЕЙ УЗЛОВ ТРЕНИЯ ВАКУУМНО-ДУГОВЫМ МЕТОДОМ

*В.А. Белоус, И.Г. Ермоленко, Ю.А. Заднепровский, Н.С. Ломино*

В целях увеличения эксплуатационного ресурса стальных деталей, представляющих собой пару трения и работающих в условиях динамической нагрузки, повышенной температуры и коррозионной среды, разработан процесс модифицирования контактирующих рабочих поверхностей с использованием вакуумно-дугового метода. Этот процесс реализован в двухстадийном технологическом цикле: упрочнение основы методом ионно-плазменного азотирования, эффективно заменяющим «печное» азотирование, и последующее осаждение защитных покрытий Mo-N и Ti-N. Исследована зависимость ряда физических свойств модифицированных образцов (профили микротвердости по глубине от поверхности, а также структурные особенности азотированных слоев и нитридных покрытий) от параметров разрабатываемого процесса. Выполнены сравнительные лабораторные испытания служебных характеристик (абразивной и коррозионной стойкости) деталей и продемонстрировано существенное улучшение этих характеристик для модифицированных поверхностей.

### КОМБІНОВАНЕ ЗМІЦНЕННЯ ДЕТАЛЕЙ ВУЗЛІВ ТЕРТЯ ВАКУУМНО-ДУГОВИМ МЕТОДОМ

*В.А. Білоус, І.Г. Єрмоленко, Ю.А. Заднепровський, М.С. Ломино*

В цілях збільшення експлуатаційного ресурсу сталевих деталей, що є парою тертя і працюючих в умовах динамічного навантаження, підвищеної температури і корозійного середовища, розроблено процес модифікування контактуючих поверхонь з використанням вакуумно-дугового методу. Цей процес реалізовано в двохстадійному технологічному циклі: зміцнення основи методом іонно-плазмового азотування, ефективно замінюючим «пічне» азотування, і подальше осадження захисних покриттів Mo-N і Ti-N. Досліджено залежність ряду фізичних властивостей модифікованих зразків (профілі микротвердості по глибині від поверхні, а також структурні особливості азотованих шарів і нитридних покриттів) від параметрів процесу, що розробляється. Виконано порівняльні лабораторні випробування службових характеристик (абразивної і корозійної стійкості) деталей і продемонстровано істотне поліпшення цих характеристик для модифікованих поверхонь.